C. R. Physique 14 (2013) 651–666

Contents lists available at ScienceDirect

Comptes Rendus Physique

www.sciencedirect.com

Disordered systems / Systèmes désordonnés

Universal magnetic domain wall dynamics in the presence of weak disorder

Universalité de la dynamique d'une paroi de domaine magnétique en présence d'un faible désordre

Jacques Ferré [a,*], Peter J. Metaxas [b], Alexandra Mougin [a], Jean-Pierre Jamet [a], Jon Gorchon [a], Vincent Jeudy [a,c]

[a] *Laboratoire de physique des solides, UMR CNRS 8502, Université Paris-Sud, 91405 Orsay, France*
[b] *School of Physics, M013, University of Western Australia, 35 Stirling Highway, Crawley, WA 6009, Australia*
[c] *Université de Cergy-Pontoise, 95000 Cergy-Pontoise, France*

ARTICLE INFO

Article history:
Available online 28 August 2013

Keywords:
Magnetic films
Wall dynamics
Creep
Depinning
Disorder

Mots-clés :
Films magnétiques
Dynamique de paroi
Reptation
Dépiégeage
Désordre

ABSTRACT

The motion of elastic interfaces in disordered media is a broad topic relevant to many branches of physics. Field-driven magnetic domain wall motion in *ultrathin* ferromagnetic Pt/Co/Pt films can be well interpreted within the framework of theories developed to describe elastic interface dynamics in the presence of weak disorder. Indeed, the three theoretically predicted dynamic regimes of creep, depinning, and flow have all been directly evidenced in this model experimental system. We discuss these dynamic regimes and demonstrate how field-driven creep can be controlled not only by temperature and pinning, but also via interactions with magnetic entities located inside or outside the magnetic layer. Consequences of confinement effects in nano-devices are briefly reviewed, as some recent results on domain wall motion driven by an electric current or assisted by an electric field. Finally new theoretical developments and perspectives are discussed.

RÉSUMÉ

Le déplacement d'interfaces élastiques dans un milieu désordonné est un sujet qui s'applique à de nombreuses branches de la physique. Le mouvement d'une paroi magnétique dans un film de Pt/Co/Pt *ultra-mince* a pu être interprété dans le cadre de théories sur la dynamique d'une interface élastique se propageant dans un milieu faiblement désordonné. Les trois régimes dynamiques prévus théoriquement, c'est-à-dire la reptation, le dépiégeage et le déplacement uniforme de la paroi, ont été directement mis en évidence dans ce système expérimental modèle. Nous discutons ici ces régimes et démontrons comment la reptation sous champ peut être contrôlée, non seulement par la température et le piégeage, mais aussi via une interaction avec des entités magnétiques situées à l'intérieur ou à l'extérieur de la couche magnétique. Les conséquences d'effets de confinement dans des dispositifs nanoscopiques sont brièvement discutées, comme certains résultats récents

* Corresponding author.
E-mail addresses: ferre@lps.u-psud.fr (J. Ferré), peter.metaxas@uwa.edu.au (P.J. Metaxas), mougin@lps.u-psud.fr (A. Mougin), jamet@lps.u-psud.fr (J.-P. Jamet), gorchon@lps.u-psud.fr (J. Gorchon), jeudy@lps.u-psud.fr (V. Jeudy).

1631-0705/$ – see front matter
http://dx.doi.org/10.1016/j.crhy.2013.08.001

sur le mouvement de paroi provoqué par un courant ou assisté par un champ électrique. Finalement, de nouveaux développements théoriques et perspectives sont proposés.

1. Introduction

Understanding the statics and dynamics of an elastic object (line, interface ...) moving in a weakly disordered media under a driving force f is of great importance for many branches in physics [1,2]. Indeed, it has been shown that interface motion in a number of different physical systems can be described within a unified concept [1]. The investigation of interface dynamics is particularly attractive when a weak driving force must compete with disorder-induced pinning effects. In magnetic materials, the force, f, is usually a magnetic field, H, that drives the motion of a magnetic domain wall (DW) separating up- and down-magnetised domains that plays the role of the interface. In this article, we will concentrate on field-driven DWs in weakly disordered *ultrathin* ferromagnetic films [3–6] with some discussion on DWs driven by an electric current [7–13] or assisted by an electric field [14–16].

DW pinning in magnetic media has traditionally been attributed to interactions between the wall and single defects [17]. As such, for systems with magnetisation reversal initiated by nucleation and field-driven DW propagation, it was proposed that walls were moving by thermal activation through successive Barkhausen jumps over local, field-independent activation energy barriers, $E_a = E_a^0 - \alpha H$, where H is the applied field. This thermally assisted flux flow (TAFF) picture [18] holds for systems with isolated hard pinning defects, but is no longer valid when the wall is moving through thin magnetic films characterised by a large assembly of weak pinning defects wherein it is pinned cooperatively by multiple defects. Alternatively, for weakly disordered *ultrathin* ferromagnetic films, it was suggested [3,19,20] that static and dynamic field-driven wall properties could be described by considering a single elastic line moving in a random environment. At low field, in the thermally activated "creep" regime, the energy barrier, $E_a \sim T_{dep}(H_{dep}/H)^{\mu}$, with μ being a universal exponent dependent on the disorder and the system's dimensionality, differs drastically from the TAFF prediction. In particular, E_a now diverges when H tends to zero and is associated with a huge slowing down. Thus, for samples with weak pinning, experimental results can be interpreted within the framework of this universal creep theory [20] that applies to many phenomena [1,2,21]. Conversely, single pinning sites can be treated by general elastic models, but do not show the universal scaling properties.

We will limit our review to recent investigations on Pt/Co/Pt *ultrathin* films or thin Co/Pt multilayers showing perpendicular magnetic anisotropy (PMA), in which the Co layer thickness is smaller than the exchange length to preserve in-depth magnetic homogeneity. Compared to films with in-plane anisotropy that show two types of transverse and vortex domains that can transform under a field, only Bloch walls are present in *ultrathin* films with PMA. The considered ferromagnetic samples may be approximated to 2D-Ising systems, the magnetisation reversal being controlled by the motion of Bloch walls separating "up" and "down" magnetised domains. This is a key condition to be able to neglect intralayer dipolar interactions for comparing results with simple statistical theories on the motion of an elastic interface in a disordered medium [1,3]. Another interesting topic, related to the stochastic Barkhausen magnetisation jumps and avalanches [22–24] and the related generation of noise [25], also due to depinning on defects [26–28], but essentially present in 3D ferromagnetic bulk samples or thick films, will not be reviewed.

Experimental results [3–5] have demonstrated that the static and dynamic magnetic properties of walls separating two domains with spin-up and spin-down magnetised domains in *ultrathin* Pt/Co/Pt ferromagnetic films with PMA are indeed well interpreted using this picture of elastic interfaces propagating through weakly disordered media. In particular, at low field, the creep law has been verified over a very wide DW velocity range, and the roughness, ζ, and dynamic, μ, exponents, were found to be in good agreement with those predicted for a 2D random disordered Ising system [3]. As predicted when increasing the field [20,29], three dynamic creep, depinning and flow regimes were unambiguously evidenced in Pt/Co/Pt films [5]. This, together with the inherent ease at which the archetypal *ultrathin* Pt/Co/Pt ferromagnetic films can be probed and manipulated, means that these systems are now one of the most investigated for testing predictions of theories for interface motion.

So, this review reports essentially on DW dynamics in isolated or magnetically coupled *ultrathin* Pt/Co/Pt films with PMA. In Section 2, the DW motion in an ideal defect-free ferromagnetic film is first considered while disorder and its relevance on DW velocities are accounted for in Section 3. Field-driven dynamic regimes are introduced in Section 4 and the influence of pertinent parameters discussed in Section 5 for single magnetic layers. The effect of coupling within the magnetic layer or between layers is examined in Sections 6 and 7. Confinement effects are discussed in Section 8. Recent experiments on current-driven and electric-field-assisted wall dynamics are reported in Sections 9 and 10. Finally, future perspectives are proposed in Section 11.

2. 1D-model of domain wall motion in a defect-free ferromagnetic layer

Field-induced magnetisation reversal in a thin magnetic film is initiated by the nucleation of small magnetically reversed regions that subsequently grow via DW propagation. A one-dimensional theoretical picture of field-driven domain wall dynamics in relatively *thick* defect-free magnetic films was developed in the second half of the 20th century by a number

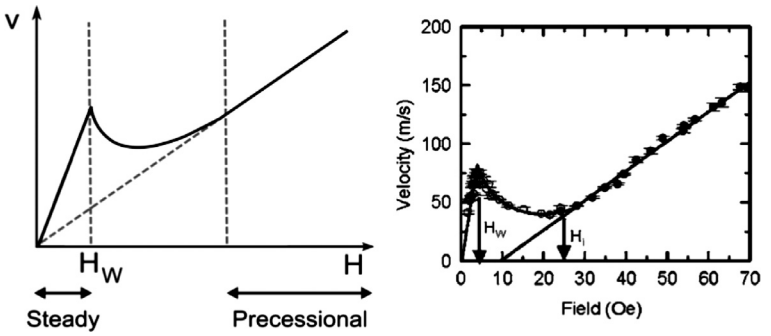

Fig. 1. (a) 1D-model theoretical prediction of the field dependence of the DW velocity in a defect-free ferromagnetic film (from [5]). (b) $v(H)$ DW velocity–field curve for a 20-nm-thick Permalloy sputtered film (from [33]).
Reprinted figure (a) with permission from P.J. Metaxas, J.-P. Jamet, A. Mougin, M. Cormier, J. Ferré, V. Baltz, B. Rodmacq, B. Dieny and R.L. Stamps, Phys. Rev. Lett. 99 (2007) 217208.

Reprinted figure (b) with permission from G.S.D. Beach, C. Nistor, C. Knuton, M. Tsoi, and J.L. Erskine, Nat. Mat. 4 (2005) 741.

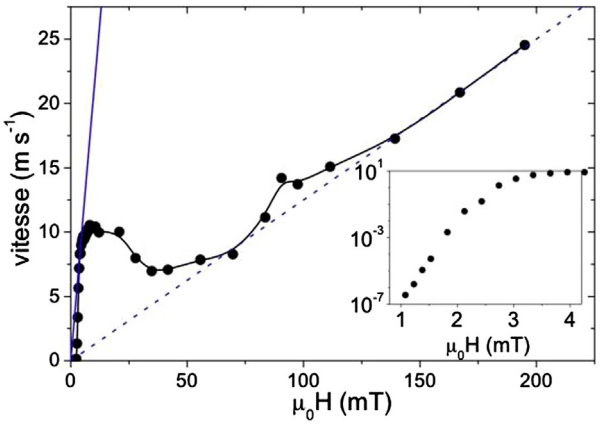

Fig. 2. DW velocity–field response curve, $v(H)$, for an epitaxially grown 50-nm-thick (GaMn)As film, measured at 80 K (from [34]). The abrupt slope indicated by a continuous line refers to the steady regime, while the dashed line slope relates to the asymptotic precessional regime. The first maximum of $v(H)$ corresponds to the Walker field anomaly that is here partly affected by disorder. In inset: plot of $\ln v$ versus the field: in this low-field range, a creep behaviour due to disorder is evidenced.
Reprinted figure with permission from A. Dourlat, V. Jeudy, A. Lemaître, and C. Gourdon, Phys. Rev. B 78 (2008) 161303R.

of authors [30–32]. Following these works, at low values of the applied field, H, the DW velocity was predicted to vary linearly with H, with a mobility, $m = v/H = \gamma\Delta/\alpha$ (γ being the gyromagnetic factor, α the damping parameter, and $\Delta = (A/K)^{1/2}$ the DW width parameter, where A is the exchange stiffness and K the magnetic anisotropy). This low-field regime is referred to at times as a steady regime since, following a brief transitory period at the onset of motion, the internal structure of the DW does not change with time as it propagates. However, beyond the so-called Walker field, $H_W = 2\pi\alpha M_s$ (M_s being the saturation magnetisation of the material), an instability of the wall structure leads to precessional magnetisation dynamics within the wall, which results in a strong reduction of its velocity. This threshold is known as the Walker breakdown [30]. Although velocity increases linearly again if the field is sufficiently large (Fig. 1a), the mobility in this last (precessional) linear regime is reduced with $m = \gamma\alpha\Delta/(1+\alpha^2)$. This characteristic behaviour was experimentally verified in a magnetically soft Permalloy ($Ni_{80}Fe_{20}$) film [33] wherein the anisotropy is weak and in the plane of the film (Fig. 1b).

The onset of Walker breakdown is directly linked to internal magnetic fields within the DW. As such, when decreasing the magnetic layer thickness, t, the Walker field is reduced by a geometrical factor related to the demagnetising fields along and normal to the wall motion [35,36]. However, the above expressions of m in the two regimes remain unchanged. In magnetic films with in-plane anisotropy, the DW width is usually large as compared to the characteristic correlation length of the disorder, ξ, meaning that pinning is not very efficient. Conversely, collective pinning generally has strong effects on the low-velocity field response in films with perpendicular anisotropy [3,5,37]. Up until now, the only exception concerns epitaxial (GaMn)As MBE grown films with large single crystallites, for which the Walker breakdown is evidenced, although superimposed onto disorder effects (Fig. 2). Obviously, the theoretical 1D-model does have some limitations in terms of

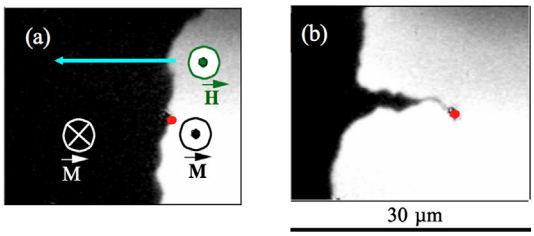

Fig. 3. Two successive (a, b) snapshots of field-induced DW motion in a Pt/Co(0.5 nm)/Pt film with transient pinning on an extrinsic defect (marked in red) (from [41] evidenced by magneto-optical Kerr microscopy). (a) The field and magnetisation directions are indicated, as well as the DW motion direction by the blue arrow. (b) As the wall touches the defect, it rolls around it and generates a thin (black) non-reversed 360° wall. Due to its high curvature energy, after some time, this wall shrinks and joins back rapidly the flat wall portion. In that case, creep can be only studied far from this defect. (For interpretation of references to colours, see the online version of this article.)
Reprinted figure with permission of J. Ferré, Spin dynamics in confined magnetic structures I, Top. Appl. Phys. 83 (2002) 127.

its applicability to complex real systems in which case dynamic micromagnetic simulations can give additional insight, as recently noted in two different types of systems, namely for thick (GaMn)As [34,38] and Co/Ni films [39].

3. Consequence of the disorder on dynamics in a single ultrathin ferromagnetic layer

The effect of disorder on field or current-driven transverse wall dynamics has been recently investigated by micromagnetic simulations on an in-plane magnetised Permalloy thin film [40] similar to that considered in Fig. 1. Some kind of collective behaviour has been modelled by considering small randomly distributed non-magnetic voids in the layer. In the field-driven case, the authors identified two efficient pinning mechanisms below and above the Walker breakdown. However, to our knowledge, no similar treatment has been proposed so far for field-driven wall motion in *ultrathin* films with PMA.

In the preceding section, the $v(H)$ response was calculated neglecting the role of defects. However, two types of defects can modify DW dynamics [41]: (i) *extrinsic* strong pinning defects related to large structurally perturbed regions of the material and (ii) *intrinsic* nanoscopic pinning defects (lattice mismatch at the boundary between crystallites or steps between atomically flat terraces in the film). Nucleations of reversed domains are initiated by *extrinsic* defects that also contribute to marked anomalies of the DW motion (Fig. 3). Depending on the magnitude of the pinning force, two classes of *intrinsic* defects have to be distinguished, the first generating rather strong pinning in non-miscible metallic multilayer films (e.g., a single magnetic layer sandwiched between two non-magnetic layers such as Au/Co/Au), and the second associated with weak pinning in films with intermixed interfaces (e.g., Pt/Co/Pt). Indeed, in Au/Co/Au films, defects are junctions between atomically flat terraces [42,43] and in that case, DW dynamics are so slow and irregular that creep is difficult to observe. Conversely, the second situation prevails in Pt/Co/Pt films, where pinning is reduced thanks to smoothening and alloying at the Co–Pt interfaces which results in creep being able to be studied over a large field range.

The outcome of these two classes of defects on the DW propagation is illustrated in Fig. 3 for a Pt/Co(0.5 nm)/Pt ultrathin film with PMA. The effect of *extrinsic* defects on wall dynamics is difficult to model in general terms, but in counterpart, *intrinsic* weak pinning defects act cooperatively to induce collective pinning on wall. Neglecting the change of the spin structure inside DWs, this motion can be understood in terms of general theories treating the motion of interfaces in disordered media [1,19,29,44–47], as supported by a number of experimental studies on Pt/Co/Pt ultrathin films [3–5,48,49].

The general velocity–force $v(f)$ behaviour displayed by an interface moving in a disordered medium (Fig. 4) has been conjectured by several authors [19,29,44]. At $T = 0$, under a driving force f smaller than the depinning force, f_c, the interface remains frozen. At very high force, in the flow regime, disorder is not efficient and v becomes proportional to f through a viscosity parameter, m. At finite temperature, walls can move slowly at low field in the creep regime, and the $v(f)$ curve exhibits thermal rounding in the depinning region. Such a general behaviour has been confirmed in ultrathin Pt/Co/Pt ferromagnetic films under magnetic field (Fig. 5) [5]. In that case, the short-range disorder is related to the non-homogeneous intermixing at Co–Pt interfaces. The three expected creep, depinning and flow regimes (Fig. 4) are clearly evidenced (Fig. 5). While DW roughness is clearly found at low field, the wall becomes smooth at high field (Fig. 5), in agreement with a reduced sensitivity to disorder.

The good agreement between theory for the motion of 1D-interfaces in 2D-media and experimental data on DW motion in Pt/Co/Pt films results from a number of unique properties of ultrathin Pt/Co/Pt films. Firstly, their high PMA generates narrow domain walls ($\Delta \sim 10$ nm), which, when coupled with the thinning down of the Co layer, leads to an excellent experimental realisation of a 2D-Ising system. Secondly, the narrow walls interact with *intrinsic* weak disorder, which is consistent with the thermally activated creep motion assumption. One consequence of this, however, is that the Walker anomaly present at low field for a perfect, defect-free film, appears to be washed out by the pinning-limited creep dynamics as schematically shown in Fig. 6 (H_W is calculated to be 170 Oe for a 0.8-nm-thick Co layer as compared to the depinning field value, $H_{dep} \gg 730$ Oe) [37]. Finally, the strong polar magneto-optical Kerr effect enables direct high-resolution imaging

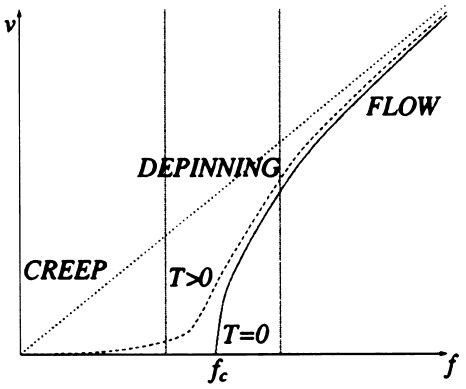

Fig. 4. $v(H)$ DW velocity–force curve prediction for an interface moving in a weakly disordered medium under a driving force f (from [20]). At $T = 0$, the interface is frozen below the threshold depinning force f_c, while the flow regime is reached at high force. At finite temperature, a creep regime is expected at low field, and the depinning regime showing thermal rounding extends around f_c.
Reprinted figure with permission of P. Chauve, T. Giamarchi, P. Le Doussal, Phys. Rev. B 62 (2000) 6241.

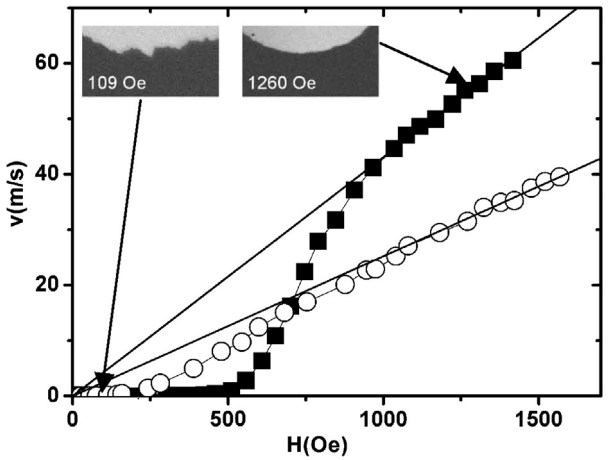

Fig. 5. Room-temperature DW velocity in two Pt/Co(0.5 nm)/Pt(○), and Pt/Co(0.8 nm)/Pt(■), ultrathin films with PMA (from [5]). Low-field creep and high-field flow regimes are clearly evidenced. The intermediate depinning regime is better revealed at higher pinning for the thicker Co(0.8 nm) layer. DW images are shown in low and high-field limits.
Figure adapted with permission from P.J. Metaxas, J.-P. Jamet, A. Mougin, M. Cormier, J. Ferré, V. Baltz, B. Rodmacq, B. Dieny and R.L. Stamps, Phys. Rev. Lett. 99 (2007) 217208.

of the DW position, thus facilitating the measurement of the wall velocity over more than ten orders of magnitude [5], enabling an accurate test of the scaling parameters that characterise the pinning energy barriers that control creep dynamics.

4. Regimes of field-driven domain wall motion

Predicted, $v(f)$, and measured, $v(H)$ DW field-driven characteristic curves were shown in Figs. 4 and 5, respectively. As already mentioned, the creep, depinning and flow regions can be distinguished when varying the magnitude of the driving force or field. These regimes have been also confirmed by susceptibility measurements over a wide frequency range [50]. More detailed experimental results obtained for Pt/Co/Pt films with PMA and their analyses are presented below for the three regimes.

4.1. The creep regime

The static roughness exponent, ζ, results from the competition of elastic and pinning forces; its universal value for a 1D-interface moving in a 2D-disordered medium has been calculated to be 2/3, in agreement with low-field results obtained for the Pt/Co(0.5 nm)/Pt film [3]. The dynamic behaviour may be also investigated in a weak driving field. It was demonstrated [20,29,44] that the DW creep velocity can be written as:

$$v = v_0 \exp\left[-\left(E_a(H,T)/k_B T\right)\right] = v_0 \exp\left[-(T_{dep}/T)(H_{dep}/H)^{\mu}\right] \quad (1)$$

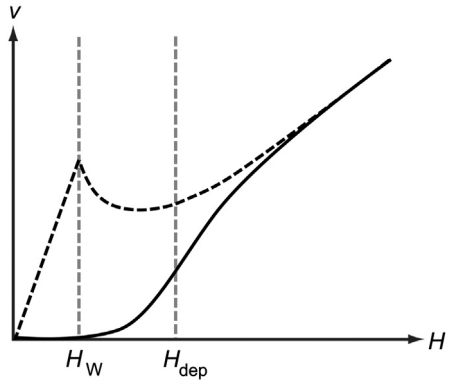

Fig. 6. Schematic illustration of the $v(H)$ behaviour in a defect-free film without disorder (dashed line) compared with the DW velocity–field curve (continuous line) deduced for the Pt/Co(0.8 nm)/Pt film (from [5]). We emphasise that disorder washes out the Walker field anomaly at H_W.
Figure adapted with permission from P.J. Metaxas, J.-P. Jamet, A. Mougin, M. Cormier, J. Ferré, V. Baltz, B. Rodmacq, B. Bieny and R.L. Stamps, Phys. Rev. Lett. 99 (2007) 217208.

E_a being the activation energy barrier and T_{dep} the associated temperature. $\mu = 1/4$ stands for the dynamic exponent for a 1D-interface moving in a 2D medium. Dynamic and static exponents are supposed to be related together through the expression $\mu = (2\zeta - 1)/(2 - \zeta)$ [20]. The pre-factor v_0 is expected to be proportional to the optimal DW jump length, L_{opt}, that is the lateral size of the thermal nucleus that subsequently trigger an avalanche [1,2].

In the case of a Pt/Co(0.5 nm)/Pt film, the expression (1) fits well low-field velocity data with $\mu \approx (0.24 \pm 0.04)$ [3] that perfectly agrees with the theoretical value of 1/4. Contrary to the TAFF regime in magnetic systems with $E_a \sim (H_{crit} - H)$ [17], the energy barrier for creep diverges at $H = 0$ (expression (1)), stabilising the domain structure at remanence, as required for long-term applications [51]. Coming back to expression (1), it has been experimentally checked [4] that the divergence of energy barriers is linked to a huge increase of avalanche sizes when reducing the field to zero. This is consistent with the associated divergence of the optimal length, L_{opt}, and with less probable events [1,46,47]. Strictly speaking, in single magnetic layers, the creep theory applies only in the absence of wall overhangs. However, creep can be investigated between far away high pinning defects (Section 2). Obviously, it does not apply for fractal percolation-like domain structures [52].

4.2. The depinning regime

At finite temperature and close below H_{dep}, the question about a dynamic criticality at the depinning transition is still debated. Some authors [53] proposed a critical behaviour just below H_{dep} with a velocity term varying like $(H_{dep} - H)^{\theta}$, while others [1,54] do not expect a "standard" critical phenomenon. In that respect, more experimental dynamic investigations have to be carried out. At finite temperature and above H_{dep}, the $v(H)$ dependence cannot be a priori easily described analytically.

4.3. The precessional flow regime

Under high driving force, the disorder is irrelevant and the interface velocity becomes proportional to the applied force with a friction coefficient describing dissipative dynamics. In magnetism, we must recover the DW velocity predicted in a defect-free system, which refers either to the steady regime (if $H_W/H_{dep} \gg 1$) or the precessional flow regime (if $H_W/H_{dep} \ll 1$). Following the above picture (Fig. 6), the disorder masks the Walker breakdown in the case of Pt/Co/Pt ultrathin films, and the high-field velocity relates to the precessional regime involving the DW width, Δ, and the damping parameter a (see Section 1) [5,35]. At low temperature and high field, it is difficult to investigate this flow regime, since the rate of nucleation of magnetic domains increases dramatically with field, preventing a clear observation of DW propagation. By enhancing the Co layer thickness in Pt/Co/Pt films, the mobility, $m = v/H$, increases [5] due to the enhancement of Δ linked to a decrease of the thickness-dependent magnetic anisotropy.

5. Field-driven creep: Adjustable parameters in single magnetic layers

5.1. Generalities

The creep law (expression (1)) is obviously sensitive to the temperature, T, to the universality class of the investigated system through the dynamic exponent μ, and to the random-bound disorder and pinning via H_{dep} and T_{dep}. Consistency with the creep law can be unambiguously checked by verifying the presence of a pure linear dependence of the natural

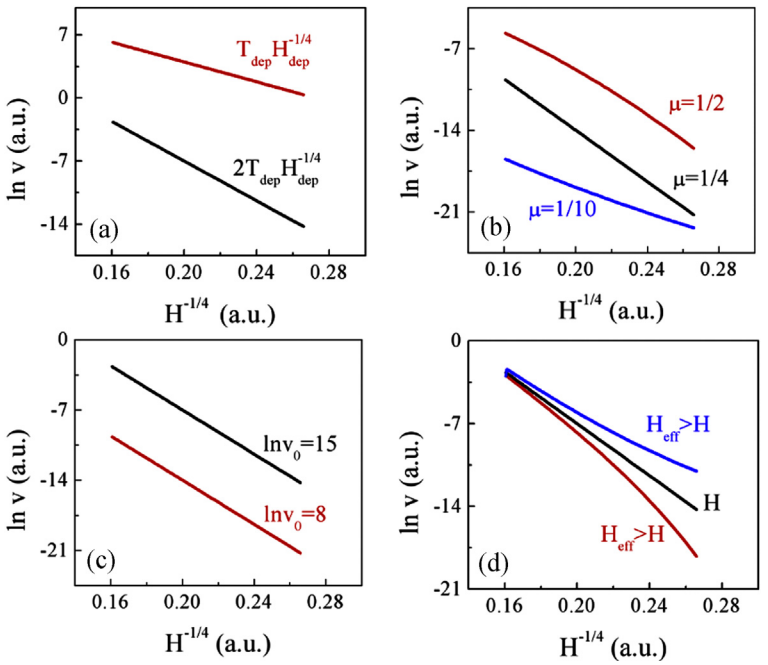

Fig. 7. Expected modifications of the creep behaviour in a $\ln v$ plot versus $H^{-1/4}$ when varying (a) H_{dep} or T_{dep}; (b) the dynamic exponent μ; (c) the value of $\ln v_0$; (d) the effective field, plotting curves for $H_{eff} = H$, and replacing H by $H_{eff} > H$, or by $H_{eff} < H$. Colour available on the web.

logarithm of the DW velocity with $H^{-\mu}$. For 2D-systems with random-bound disorder, $\mu = 1/4$, and expected modifications to the creep dynamics are represented in Fig. 7 in a $\ln v$ against $H^{-1/4}$ plot. The influence of the disorder can be checked from the creep slope, which is proportional to $T_{dep}\ H_{dep}^{1/4}$ (Fig. 7a). The departure from the value $\mu = 1/4$ can be tested from the plot curvature (Fig. 7b). However, to obtain a value of μ with a good accuracy, dynamics must be investigated over a wide range of DW velocities (multiple orders of magnitude). The crossing point of the velocity curve with the $H = 0$ axis gives access to $\ln v_0$ (Fig. 7c). As we shall see below, in case of magnetic interaction with another layer, the applied field, H, has to be replaced by an effective field, H_{eff}, in which case deviation from a pure $H^{-1/4}$ law is anticipated (Fig. 7d). However, a plot of $\ln v$ against $H_{eff}^{-1/4}$ restores linearity. In the following, the roles of several parameters are examined.

5.2. The temperature

The creep phenomenon is obviously very sensitive to temperature. Refined analyses were carried out recently on a Pt/Co(0.45 nm)/Pt film taking into account the temperature dependence of all pertinent parameters [55]. The creep law was verified between 50 K and 300 K. By lowering the temperature, the slope of the $\ln v(H^{-1/4})$ increases markedly as a result of the reduction of T/T_{dep} (see Eq. (1)). Under cooling, the quantity T/T_{dep} controls the thermal rounding in the creep and depinning regions (expression (1)) [45,55]. A low value of the thermal rounding exponent, consistent with numerical simulations, $\psi = 0.15$ [45,56], was obtained. Previous dynamic analyses did not consider the thermal dependence of all pertinent quantities [57], such as H_{dep} and T_{dep}. Conversely, H_{dep} was found to increase significantly when lowering the temperature in both Co/Pt multilayers [58] and Au/Co/Au films [59].

5.3. Varying the creep energy barrier via modifications to the domain wall pinning within a layer

As mentioned in Section 3, it is generally assumed that DW pinning is associated with local variations of magnetic parameters (exchange stiffness, A, and anisotropy, K) that control DW pinning at the boundary between nano-crystallites or at steps between atomic terraces. An increase of the Co layer thickness can favour the formation of de-correlated regions, which tends to increase DW pinning. As a consequence, H_{dep} and T_{dep} increase with the Co layer thickness, consistently with the increased gradient in the creep data shown in Fig. 8 [5]. Empirically, it is also seen that $\ln v_0$ is highly dependent on the film structure and presumably the resulting disorder. Finally, we note that sophisticated scaling analysis of data obtained in films with different thickness recently enabled the experimental determination of a value for the thermal rounding exponent, $\psi \approx 0.2$, which was notably consistent with numerical simulations [49] and results from measurements at variable temperatures [55].

He^+ ion irradiation of ultrathin Pt/Co/Pt films can reinforce the formation of Co–Pt alloys at interfaces, thereby reducing the magnetic anisotropy and DW pinning in a controlled way [60,61]. For a Pt/Co(0.5 nm)/Pt film uniformly irradiated

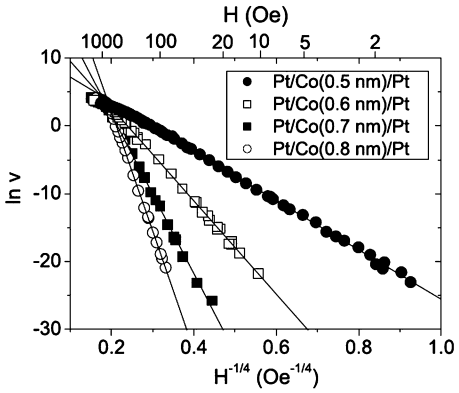

Fig. 8. Natural logarithm of the DW velocity for Pt/Co/Pt films with four different Co thicknesses plotted against $H^{-1/4}$ that agrees with the creep theory prediction (from [5]).
Figure adapted with permission from P.J. Metaxas, J.-P. Jamet, A. Mougin, M. Cormier, J. Ferré, V. Baltz, B. Rodmacq, B. Bieny and R.L. Stamps, Phys. Rev. Lett. 99 (2007) 217208.

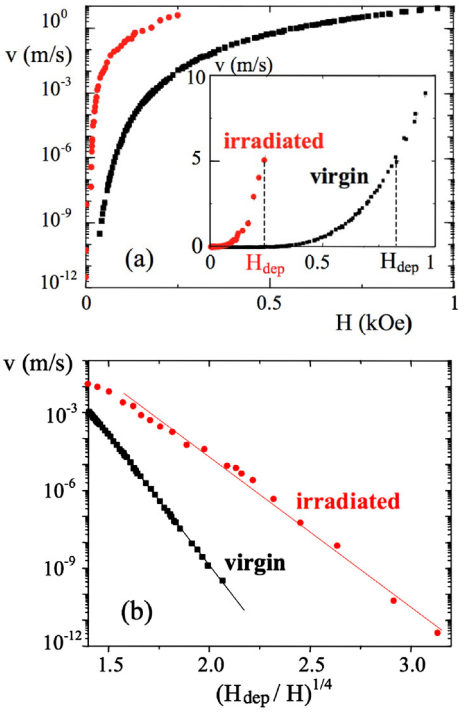

Fig. 9. (a) Semi-logarithmic plot of the DW velocity against the applied field for a virgin and irradiated ($F = 10^{16}$ Ga^+ ions/cm^2) Pt/Co(0.5 nm)/Pt film. In inset: $v(H)$ linear plot for the same samples (from [60]). (b) Plot of v versus $(H_{dep}/H)^{1/4}$ to reveal the creep behaviour. Colour available on the web.
Figure adapted with permission of J. Ferré, V. Repain, J.-P. Jamet, A. Mougin, V. Mathet, C. Chappert and H. Bernas, Phys. Stat. Sol. A 201 (2004) 1386.

by He^+ ions under a moderate fluence, scaling of the pinning energy barriers remains consistent with creep. However, H_{dep} is lowered by a factor 3.5 (Fig. 9a, inset) and, from the plots in Fig. 9b, it can be deduced that T_{dep} is reduced by about 20%. Irradiation reduces the coercivity and depinning field, thus enhancing wall motion in DW devices, something that is important for spintronic applications. Localised ion irradiation has also been used to design micron-wide tracks in Pt/Co(0.5 nm)/Pt films [62] and create periodic pinning potentials (e.g., [63]).

6. Field-driven domain wall motion: interactions within the layer

We have seen above that it was possible to act on DW creep dynamics in a single magnetic layer by adjusting internal parameters. The purpose of the present section is to examine modifications to DW motion in a given ultrathin ferromag-

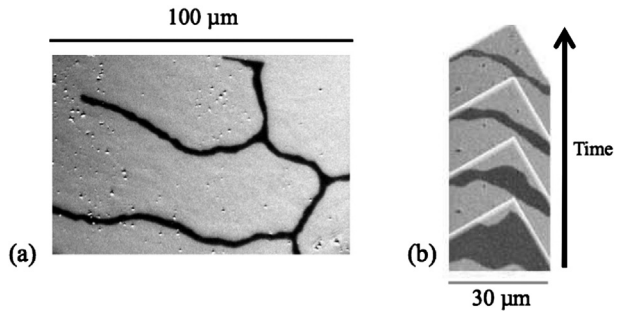

Fig. 10. Uniformly He^+ ion irradiated Pt/Co(0.5 nm)/Pt film ($F = 10^{16}$ He ions/cm^2). (a) Stabilised 360° non-reversed DWs (in black) at long time under $H = 1$ Oe. (b) Time evolution (from the bottom to the top) of the strip domain (in black) separating the two reversed domains (in grey) (from [65]).
Figure (b) adapted with permission from M. Bauer, A. Mougin, J.-P. Jamet, V. Repain, J. Ferré, R.L. Stamps, H. Bernas, and C. Chappert, Phys. Rev. Lett. 94 (2005) 207211.

netic layer due to the coupling to a strain potential [65] or magnetostatic interactions with another wall inside the same layer [64].

Long-range magneto-elastic interaction of a DW with a correlated linear defect can drastically perturb its field-driven creep motion, as shown in a Pt/Co(0.7 nm)/Pt ultrathin film with PMA [64,66]. In this work, a linear defect produced by focused Ga^+ ion beam patterning created a 1D-strain-induced effective potential variation, which was competing with the intrinsic disorder. As a result, and due to the strain gradient, the wall slows down progressively and is submitted to a kinetic deroughning over a longer length as the DW approaches the defect. Creep has to account for this additional long-range variable interaction. Consequently, the roughness exponent ζ varies from 0.6 (its value being $\zeta = 2/3$ in the non-patterned film area) to a much lower value, $\zeta = 0.1$, for a wall located close to the linear defect. Indeed, a new characteristic elastic length arises from the competition between the magneto-elastic and Zeeman energies. It was originally proposed that such strain effects could be used for applications requiring the stabilisation of domains in confined regions [64].

In magnetic films with PMA, the dipolar interaction can inhibit the merging of two neighbouring aligned magnetic domains, creating 360° domain wall strips at long time (Fig. 10a). This phenomenon has been observed and analysed in a uniformly He^+ irradiated ultrathin Pt/Co(0.5 nm)/Pt film [65]. The irradiation fluence, $F = 10^{16}$ He^+ ions/cm^2, was chosen to significantly reduce the depinning field and the coercivity, the latter down to 5 Oe. As two de-correlated Bloch walls approach each other in this system under a fixed small field, they tend to smooth over long distances to finally become nearly parallel (Fig. 10b). Since the dipolar interaction can be exactly calculated, this system was well adapted to a quantitative analysis of the de-roughening phenomenon. The creep theory was modified to include dipolar interactions between domains during which a new characteristic dipolar length was defined.

7. Field-driven domain wall motion in magnetically coupled layers

The purpose of this section is to sum up and compare studies on DW dynamics in Pt/Co(0.5 nm)/Pt(x nm)/Co(0.8 nm)/Pt containing two coupled magnetically soft (Co(0.5 nm)) and hard (Co(0.8 nm)) ferromagnetic layers [37]. A number of coupling mechanisms can contribute to interlayer magnetic coupling, ranging from magnetostatic coupling via stray magnetic fields at domain boundaries [67] to orange-peel and RKKY-like interlayer interactions [68]. The effect of an interlayer interaction, J, is usually interpreted in term of an effective coupling field, $H_J = J/M_s t$, where M_s and t are, respectively, the saturation magnetisation and the thickness of the layer subject to the coupling-induced effective field [69]. This effective coupling field not only can drive DW motion, but also can generate interactions between walls existing in physically separated, but magnetically coupled layers, thereby offering a method to experimentally study the dynamics of coupled interfaces, here moving in distinct media with different disorder realisations. A good degree of coupling tunability is also possible in such systems. Indeed, by changing the thickness, x, of the Pt spacer layer, the effective interaction between two Co layers can be either antiferromagnetic ($x = 4$ nm) [67,70], or ferromagnetic ($x = 3$ nm) [71], the latter (former) favouring an alignment (anti-alignment) of the magnetisation vectors in each layer.

A simple example of the consequences of an effective coupling field can be seen when studying DW motion in a magnetic layer which is coupled to a second, uniformly magnetised layer across a 4-nm Pt spacer (weak antiferromagnetic coupling) [70]. In this case, the effective coupling field acting on the first layer can be considered to be spatially uniform. Depending on the polarity of the applied field, H, the effective coupling field will then either oppose or reinforce H. In Fig. 11, we show the consequence of this effect: walls move faster for positive H than for negative H, which is consistent with a positive coupling field. Furthermore, as expected (Fig. 7d), creep plots of $\ln v$ against $|H|^{-1/4}$ are non-linear due to the additional coupling field, displaying opposite curvatures for the two field polarities. However, linear data are recovered and the two curves for $H > 0$ and $H < 0$ superimposed on one another when plotting $\ln v$ against $|H_{\text{eff}}|^{-1/4} = |H + H_J|^{-1/4}$, i.e. a modified creep law, with $H_J = 4.9 \pm 1.2$ Oe (Fig. 11, inset), a value consistent with that extracted independently from

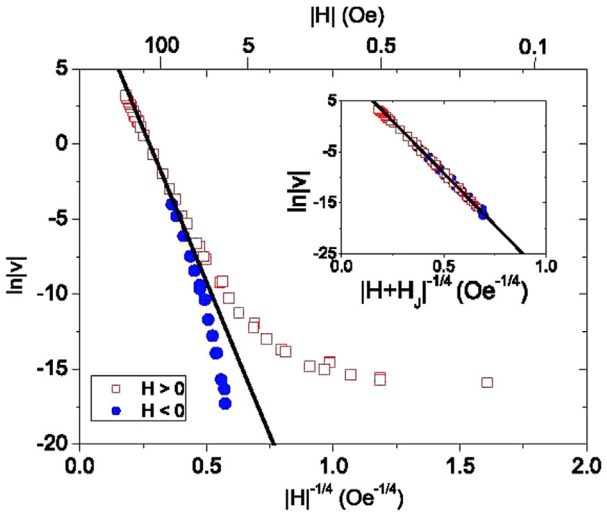

Fig. 11. Natural logarithm of the wall velocity in the antiferromagnetically coupled soft layer plotted against $|H|^{-1/4}$ for positive or negative applied fields. The inset shows the same $\ln|v|$ data plotted against $|H + H_J|^{-1/4}$ with $H_J = 4.9$ Oe. The linear fit for $|H + H_J| = 300$ Oe is shown as a solid line with gradient: $T_{\text{dep}} H_{\text{dep}}^{1/4} = -40$ K Oe$^{1/4}$ (from [70]). Colour available on the web.

Reprinted figure with permission of P.J. Metaxas, J.-P. Jamet, J. Ferré, B. Rodmacq, B. Dieny, and R.L. Stamps, J. Magn. Magn. Mater. 320 (2008) 2571.

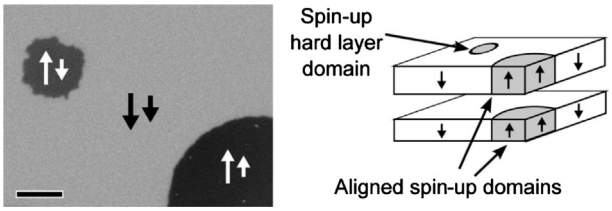

Fig. 12. Magneto-optical image and corresponding sketch of magnetic domains in a Pt/Co(0.5 nm)/Pt(3 nm)/Co(0.8 nm)/Pt film with PMA following nucleation and DW propagation under a positive field pulse [71]. The long (short) arrow corresponds to the magnetisation direction in the 0.8 nm (0.5 nm) thick Co layer. The black scale bar is 10 mm long. It is non-trivial to compare the roughness of the two domain walls since the aligned and isolated DWs are subject to different net driving fields resulting in different contributions from the disorder-induced pinning.

Reprinted figure with permission from P.J. Metaxas, R.L. Stamps, J.-P. Jamet, J. Ferré, V. Baltz, B. Rodmacq, and P. Politi, Phys. Rev. Lett. 104 (2010) 237206.

minor hysteresis loop shifts. This confirms the validity of the modified creep law, preserving the exponent $\mu = 1/4$ when replacing $|H|$ with $|H_{\text{eff}}|$.

For thinner Pt spacer layers ($x = 3$ nm), ferromagnetic interlayer coupling arises, which generates attractive domain wall interactions. These can subsequently lead to DWs in separate layers being bound together dynamically during field-driven motion [71]. Fig. 12 shows a magneto-optical image of domain structures in a Pt/Co(0.5 nm)/Pt(3 nm)/Co(0.8 nm)/Pt film with ferromagnetic interlayer coupling. Thanks to convenient extrinsic defects, it was possible to nucleate magnetic domains which existed in one layer only ("isolated") or in both layers with aligned domain walls (see Fig. 12). Similarly to the sample discussed above, the motion of isolated DWs could be used to determine the strength of the interlayer coupling, $H_J = 220$ Oe (120 Oe) acting on the Co(0.5 nm) (Co(0.8 nm)) layer.

The velocity–field response of DWs in the Co(0.5 nm) and Co(0.8 nm) layers in the absence of coupling are shown in Fig. 13a (note that experimental constraints meant that the dynamics in the Co(0.5 nm) layer had to be measured in another similar multilayer film). The main point to note is that the two $v(H)$ curves cross at two points, $H = 0$ and $H = H^*$. The first one is a universal crossing point (i.e. any two interfaces or DWs will have $v = 0$ in the absence of a driving force), whereas the second crossing point arises as a result of the thickness-dependent DW dynamics (Section 5.3). The attractive DW interactions in this system mean that in the neighbourhood of these crossing points (i.e. in field ranges wherein the wall velocities are already *similar*), walls in the two layers actually move together in a dynamically bound state. From studying the dynamics of aligned domains (Fig. 12), it was possible to experimentally determine [71,72] field ranges for these bound states (Fig. 13a, marked as "B") as well as the velocity–field response of these bound walls. The first bound state indeed arises at low field near $H = 0$, with the second being close to the high-field crossing point ($H = H^*$). Outside the bound-state field regions, the velocities of the walls are too different for the finite domain wall coupling to keep them bound, one domain wall leading the other. Within the bound-state field ranges, however, the walls move at a common velocity, which is notably distinct from the velocities of isolated walls in the Co(0.5 nm) and Co(0.8 nm) layers

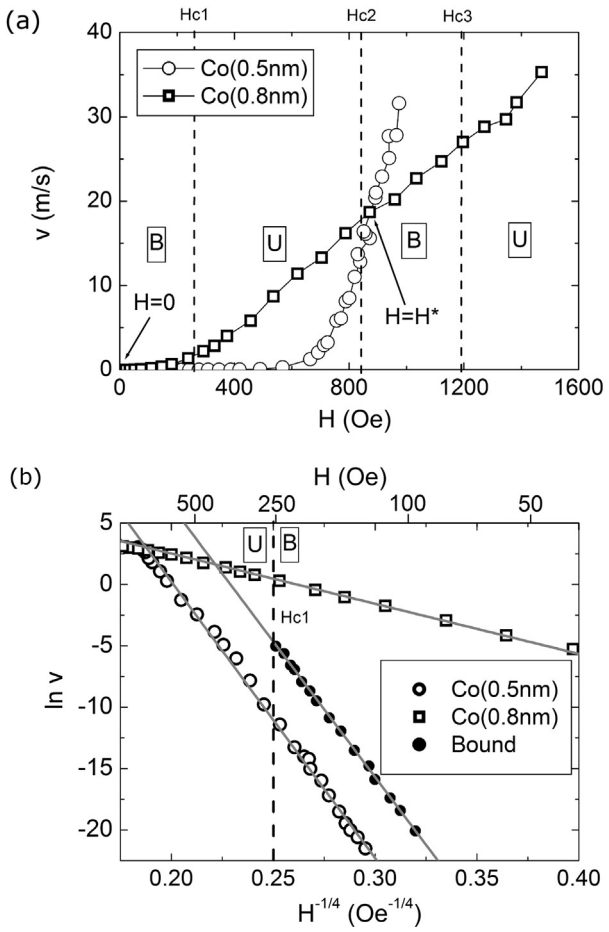

Fig. 13. (a) "Isolated" (zero-coupling case) DW velocity–field responses in Co(0.5 nm) and Co(0.8 nm) layers within a ferromagnetically coupled multilayer. Field-ranges for bound (B) or unbound (U) walls during motion are shown. (b) Velocity of bound DWs compared to isolated DWs (from [72]).
Figure adapted with permission from P. Politi, P.J. Metaxas, J.-P. Jamet, R.L. Stamps, and J. Ferré, Phys. Rev. B 84 (2011) 054431.

(Fig. 13b). Notably, the bound-state field range and bound velocity near $H = 0$ can be reproduced with good accuracy using a 1D-model [72].

8. Field-driven motion in confined geometries

Requirements for tightly controlled DW propagation pathways, the ability to use current to drive wall motion and the need to integrate storage and spintronic devices [73,74] into miniaturised electronic circuits means that wall motion must be understood not only in continuous films (the focus of this article up until this point), but also in nanostrip geometries wherein the wall moves back and forward along a patterned ferromagnetic strip.

In such systems, there are clearly practical concerns such as DW pinning induced by patterning and unintended patterning-generated defects. In studies on relatively wide wires (on the order of $w = 1$ μm) the conventional $\mu = 1/4$ energy barrier scaling is generally maintained [75] with a potential for modifications to the size of the energy barrier rather than its scaling with the applied field H. Indeed, studies on systems with controlled edge roughness have also established direct links between edge roughness and modified pinning parameters (e.g., T_{dep}, H_{dep}) [75].

Perhaps even more interesting however is that nano-patterned systems can be used to study fundamental phenomena such as dimensionality crossover. In a landmark paper on DW creep dynamics in sub-micron Pt/Co(0.3 nm)/Pt strips, Kim et al. demonstrated a change in the energy barrier scaling which was indicative of a 2D to a 1D transition [6] (Fig. 14). The $v(H^{-1/4})$ 2D-creep law is still verified down to a few Oe if the nanowire width does not exceed $w = 500$ nm (Figs. 14a–d). However, for narrower nanowires (Figs. 14e–h), the creep law was invalidated at low-field and a 1D-hopping process [76] suggested. The ratio between the strip width and the Larkin length, L_C (defined from the equality between the elastic and pinning energies) then controls this dimensionality crossover. This is entirely consistent with the original idea of a wall displacement with rigid segments of length L_C [3].

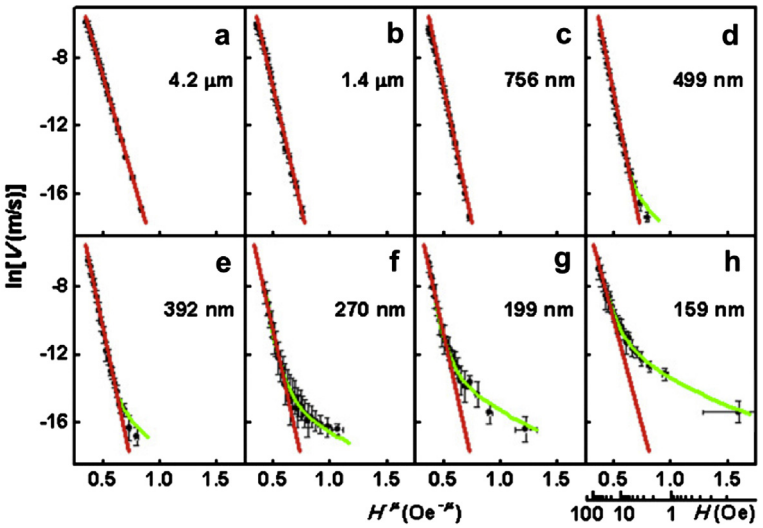

Fig. 14. Creep plots of the natural logarithm of the DW velocity against $H^{-1/4}$ (here $\mu = 1/4$) in Pt/Co (0.3 nm)/Pt film nanowires with widths, w, indicated in (a) to (h) windows. The straight line (in red) corresponds to the creep fit, while the low-field curved line (in green) indicates a hopping process (from [6]). Colour available on the web.

Reprinted figure with permission from K.-J. Kim, J.-C. Lee, S.-M. Ahn, K.-S. Lee, Y.-J. Cho, S. Seo, K.-H. Shin, S.-B. Choe, and H.W. Lee, Nature 458 (2009) 740.

9. Electric-current-driven wall motion

Approximately 30 years ago, it was predicted that an electrical current could be used to move DWs via what is now commonly known as the spin transfer torque (STT) mechanism. This has been incredibly exciting for those working in the field of spintronics, opening the way for addressable, scalable, non-volatile, high-speed, high-density, and low-energy spintronic devices based upon DWs [63,74,77,78]. For current-driven DW motion, the angular momentum of a spin-polarised current is transferred to the spins within the DW, resulting in a torque which can move and/or deform the DW. This effect has recently attracted much attention and many groups have investigated current-driven DW motion in thin film patterned micro- or nanowires, often making comparisons with field-driven measurements (e.g., [79–81]). A spin-polarised current can affect DWs through either adiabatic or non-adiabatic contributions. For example, the spin of the electron can adiabatically "track" the local spin orientation as it traverses the DW; however, while the adiabatic torque distorts the DW structure, it cannot drive steady motion. Conversely, the non-adiabatic torque applied on the wall can displace it along the wire in the same way as an effective field [7–9].

The first current-driven wall motion measurements were performed in thin films with in-plane magnetic anisotropy. For thin (20 nm) $Ni_{80}Fe_{20}$ Permalloy films [82], it was necessary to simultaneously apply an external field to favour DW depinning, after which the current could be used to drive a rather stochastic domain wall motion. The general shape of the averaged $v(H)$ characteristic curve (Fig. 1b) is not significantly modified under current with the current-induced contribution to the conventional field-driven DW velocity varying linearly with the current density up to 6×10^{11} A/m^2.

Micromagnetic simulations have demonstrated [83,84] that films with PMA might be better candidates than films with in-plane anisotropy because of the higher anisotropy and narrower DWs, the possible reduction of the threshold current density minimising Joule heating drawbacks. Non-adiabatic STT is more efficient in systems with narrow walls. Thus, many recent works concentrated on films with PMA in spite of the fact that pinning usually affects more nucleation.

Selected metallic Pt/Co/Pt ultrathin ferromagnetic films [48,85], and epitaxial (GaMn)As [86,87] magnetic semiconductor films can display PMA. (GaMn)As is an archetypal system for the study of current-driven effects, since pinning is weak both for nucleation and DW propagation, magnetisation is low just below the Curie temperature, so purely current-driven DW creep motion has been measured even at low current density ($J = 5 \times 10^9$ and 5×10^8 A/m^2, respectively) making easier the data analysis and limiting spurious Joule heating effects. At such low current values, measurements are very repetitive. Conversely, for Co/Pt multilayers, pinning plays a large role in determining the DW dynamics with the majority of the current-induced results being obtained under field [81,88,89] or heating [90], or more generally focused on depinning [13,91,92].

Although steady DW motion is predicted to come from the non-adiabatic STT term, a complete understanding of the underlying physical processes remains quite elusive (e.g., [93]). The STT efficiency relates undoubtedly to spin–orbit coupling and spin dynamic structure inside DWs. Depending on the studied system, the spin–orbit related Rasbha [10,81] or spin–Hall [13,94] effects have been invoked to interpret large STT efficiency in non-centrosymmetric thin film structures [89]. These effects are supposed to stabilise the Bloch DW structure. Additionally, Thiaville et al. [95] suggested recently that

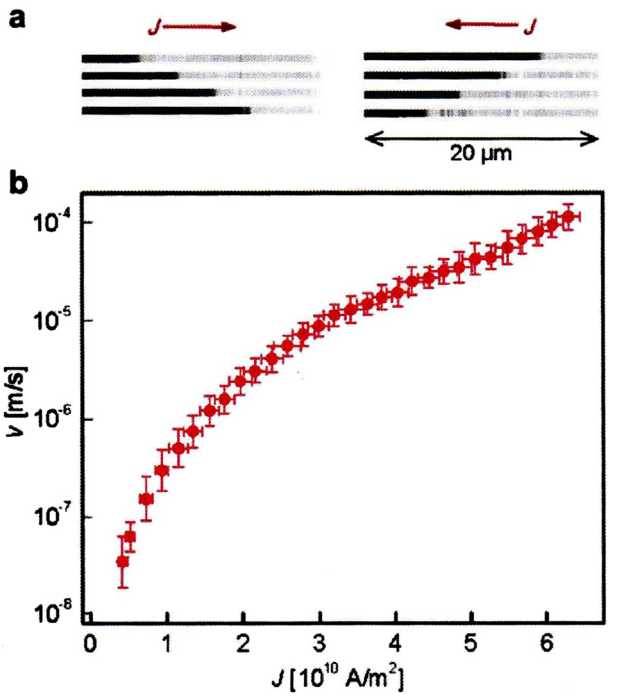

Fig. 15. (a) PMOKE images of the magnetisation in the nanowire taken after each current pulse ($J = \pm 3.1 \times 10^{10}$ A/m^2). The arrows indicate the direction of the current. (b) Current-driven DW velocity, v, against the current density, J, for a 860-nm-wide Pt/Co(0.3 nm)/Pt nanowire [85]. The symbols show averaging of 50 repeated measurements for each J value. The slight increase of v at high field is due to Joule heating.
Reprinted figure with permission from K.-J. Kim, J.-C. Lee, K.-H. Shin, H.-W. Lee, and S.-B. Choe, Current Appl. Phys. 13 (2013) 228.

a new type of Dzyaloshinskii DW could play an important role in increasing wall stability for current-driven wall motion in non-centrosymmetric ultrathin magnetic films with PMA.

Electric-current-driven DW results were recently obtained on a Pt/Co(0.3 nm)/Pt *ultrathin* film [85] (Fig. 15). After a field-current normalisation, they can be superimposed to the same field-driven $v(H)$ curve, except at high current, where a weak Joule heating effect has to be taken into account [6,48,85]. Thus, they concluded that the non-adiabatic torque was essentially involved, and that the field- and current-driven phenomena were belonging to the same universality class. A similar more qualitative result has been also reported for a Pt/Co/AlO$_x$ film [81] or a Co/Pt multilayer [96]. In this last case, a modified expression of the creep law was proposed:

$$v = v_0 \exp\left[-\left(T_{\text{dep}}/\left(T + bJ^2\right)\right)\left(H_{\text{dep}}/H + aJ\right)^{\mu}\right] \tag{2}$$

which takes the STT (aJ) and thermal Joule (bJ^2) effects into account separately.

In conclusion, the similarity between μ exponents for field- and current-driven effects demonstrates that they both belong to the same universality class in such metallic magnetic films with random-bound disorder. This apparently differs from what was found for the (GaMn)As magnetic semiconductor where the creep law seemed to be fulfilled with drastically different exponents $\mu_H = 1.2$ and $\mu_J = 0.33$ from $\mu = 1/4$ [97]. The authors concluded that an adiabatic STT was active, an explanation which is in contradiction with theoretical predictions and more recent (H, J) velocity measurements [87]. Additionally, note that similar confinement effects in nano-tracks were found for current or field [85].

10. Electric-field-assisted wall motion

The electric control of the magnetic anisotropy was first demonstrated in the (GaMn)As magnetic semiconductor [14], but no magnetisation dynamics studies under an electric field have been reported so far in this system. Only a few results on the change in DW velocity under an electric field have been reported recently in metallic thin films with PMA [15,16]. The influences of gate voltage, temperature and field on the DW creep dynamics have been investigated in Pt/Co/AlO$_x$, Pt/CoB/TaO$_x$ [15] and Pt/Co/GdO$_x$ films [16]. Here the PMA is found to scale linearly with the applied voltage, V, the change of the surface anisotropy being at the origin of the DW velocity to the applied voltage. It has been suggested that electric control of the DW motion could be exploited to build new spintronic devices [15].

11. Conclusion and perspectives

We have demonstrated that ultrathin ferromagnetic films with PMA, essentially Pt/Co/Pt films, are ideal candidates to verify and test universal theoretical predictions concerning the statics and dynamics of a single elastic structure embedded in a weakly disordered medium. DWs in ultrathin films mimic 1D-elastic entities well because they are usually narrower than the correlation length of the disorder. As opposed to other experimental model systems, they are both easy to probe and manipulate, the latter via magnetic field or injected current. Furthermore, the theoretically predicted creep, depinning and flow regimes have been clearly identified and studied in these ultrathin magnetic films [3,5]. The predicted creep regime has been experimentally confirmed over many decades of DW velocities, surviving up to rather high magnetic fields (often up to $0.8H_{\mathrm{dep}}$). Diverging energy barriers are found in the creep regime as the driving force amplitude diminishes towards zero. Several parameters, i.e. the temperature, film morphology, and structure at the interface can be adjusted to tune or control the pinning energy barriers. The effects of magnetic or magneto-elastic couplings inside the magnetic layer or between layers are reported. For magnetically coupled layers, the creep law was still valid when replacing H by an effective field that accounts for interlayer interactions. Confinement below a few Larkin lengths results in a transition between a 2D-creep and a 1D-hopping process, both for field- and current-driven wall motion.

Among the open questions concerning creep, it would be of interest to investigate non-equilibrium behaviour and ageing effects at very small driving field amplitudes as well as the significance and thermal dependence of the dynamic prefactor, v_0 (expression (1)). There is also some contradictory claims about the universality classes and creep exponents for field- and current-induced effects in 2D-systems which are characterised either by short- or long-range disorder and interactions [87,97,98]. This might be clarified by orienting future experiments on systems that are representatives of distinct universality classes.

More experimental and theoretical results must also be carried on the critical aspect of the depinning transition at finite temperature, especially below the field depinning threshold, H_{dep}. The thermal rounding behaviour of $v(H)$ and the related ψ exponent [45] might be checked experimentally. In order to improve the interpretation of the results obtained for disordered *ultrathin* magnetic films with PMA at finite temperature, it would be important to take into account the DW's internal magnetic structure as well as its dependence on the applied field or injected current. Only few attempts have been reported in this respect [99,100]. As for films with in-plane anisotropy [40], simulations including a random disorder would be of great interest for identifying pinning mechanisms in films with PMA that strongly modify the velocity–field and velocity–current responses [10].

Spintronic applications also make an understanding of field- and current-driven DW motion in films with PMA extremely important. The study of DW dynamics in the presence of pinning and various types of interactions are required both for a better knowledge of fundamental physics and for designing new spintronic devices, magnetic memories and recording media. Moreover, patterned nano-structures can serve to verify statistical theories. For example, more and more experimental studies are being carried out, not only on nanowires, but also on films and nano-structures subject to artificial, spatially periodic pinning potentials [58,61,63,101–103]. In spite of an increasing number of experimental contributions in this latter field, related theoretical studies remain quite low [104–106].

Acknowledgements

The authors acknowledge V. Baltz and B. Rodmacq for providing us well adapted samples for dynamic studies. The authors also wish to thank S. Bustingorry, T. Giamarchi, R.L. Stamps, P. Politi and A. Thiaville for fruitful discussions and collaborations. This work was partly supported by the French-Argentine project ECOS-Sud No. A12E03 and by the French project DIM C'Nano IdF. P.J.M acknowledges support from the University of Western Australia and the Australian Research Council's Discovery Early Career Researcher Award scheme (DE120100155).

References

[1] E. Agoritsas, V. Lecomte, T. Giamarchi, Phys., B Condens. Matter 407 (2012) 1725.
[2] E.E. Ferrero, S. Bustingorry, A.B. Kolton, A. Rosso, C. R. Physique (2013), in this issue.
[3] S. Lemerle, J. Ferré, C. Chappert, V. Mathet, T. Giamarchi, P. Le Doussal, Phys. Rev. Lett. 80 (1998) 849.
[4] V. Repain, M. Bauer, J.-P. Jamet, J. Ferré, A. Mougin, C. Chappert, H. Bernas, Europhys. Lett. 68 (2004) 460.
[5] P.J. Metaxas, J.-P. Jamet, A. Mougin, M. Cormier, J. Ferré, V. Baltz, B. Rodmacq, B. Dieny, R.L. Stamps, Phys. Rev. Lett. 99 (2007) 217208.
[6] K.-J. Kim, J.-C. Lee, S.-M. Ahn, K.-S. Lee, C.-W. Lee, Y.-J. Cho, S. Seo, K.-H. Shin, S.-B. Choe, H.W. Lee, Nature 458 (2009) 740.
[7] S. Zhang, Z. Li, Phys. Rev. Lett. 93 (2004) 127204.
[8] G. Tatara, H. Kohno, Phys. Rev. Lett. 92 (2004) 086601.
[9] A. Thiaville, Y. Nakatani, J. Miltat, Y. Suzuki, Europhys. Lett. 69 (2005) 990.
[10] E. Martinez, Adv. Condens. Matter Phys. 2012 (2012) 954196.
[11] G.S.D. Beach, M. Tsoi, J.L. Erskine, J. Magn. Magn. Mater. 320 (2008) 1272.
[12] M. Yamanouchi, J. Ieda, F. Matsukura, S.E. Barnes, S. Maekawa, H. Ohno, Science 317 (2007) 1726.
[13] P.P.J. Haazen, E. Murè, J.H. Franken, R. Lavrijsen, H.J.M. Swagten, B. Koopmans, Nat. Mater. 12 (2013) 299.
[14] D. Chiba, M. Sawicki, Y. Nishitani, Y. Nakatani, F. Matsukura, H. Ohno, Nature 455 (2008) 515.
[15] A.J. Schellekens, A. van den Brink, J.H. Franken, H.J.M. Swagten, B. Koopmans, Nat. Comm. 3 (2012) 847.
[16] U. Bauer, S. Emori, G.S.D. Beach, Appl. Phys. Lett. 101 (2012) 172403.
[17] P. Gaunt, Philos. Mag. B 48 (1983) 261.

[18] P.W. Anderson, Y.B. Kim, Rev. Mod. Phys. 36 (1964) 39.
[19] T. Nattermann, Y. Shapir, I. Vilfan, Phys. Rev. B 42 (1990) 8577.
[20] P. Chauve, T. Giamarchi, P. Le Doussal, Phys. Rev. B 62 (2000) 6341.
[21] P. Paruch, et al., C. R. Physique (2013), in this issue.
[22] P. Cizeau, S. Zapperi, G. Durin, E. Stanley, Phys. Rev. Lett. 79 (1997) 4669.
[23] G. Durin, S. Zapperi, Phys. Rev. Lett. 84 (2000) 4705.
[24] D.-H. Kim, S.-B. Choe, S.-C. Shin, Phys. Rev. Lett. 90 (2003) 087203.
[25] E. Puppin, Phys. Rev. Lett. 84 (2000) 5415.
[26] J.S. Urbach, R.C. Madison, J.T. Markert, Phys. Rev. Lett. 75 (1995) 276.
[27] G. Bertotti, in: Hysteresis in Magnetism, Academic Press, San Diego, CA, 1998.
[28] G. Durin, S. Zapperi, in: G. Bertotti, I. Mayergoyz (Eds.), The Science of Hysteresis, Academic Press, Amsterdam, 2006, pp. 181–267.
[29] S. Brazovskii, T. Nattermann, Adv. Phys. 53 (2004) 177.
[30] J.C. Slonczewski, Int. J. Magn. 2 (1972) 85.
[31] N.L. Schryer, L.R. Walker, J. Appl. Phys. 45 (1974) 5406.
[32] A.P. Malozemoff, J.C. Slonczewski, in: Magnetic Domain Walls in Bubble Materials, Academic Press, New York, 1979.
[33] G.S.D. Beach, C. Nistor, C. Knutson, M. Tsoi, J.L. Erskine, Nat. Mater. 4 (2005) 741.
[34] A. Dourlat, V. Jeudy, A. Lemaître, C. Gourdon, Phys. Rev. B 78 (2008) 161303.
[35] A. Mougin, M. Cormier, J.-P. Adam, P.J. Metaxas, J. Ferré, Europhys. Lett. 78 (2007) 57007.
[36] D.G. Porter, M.J. Donahue, J. Appl. Phys. 95 (2004) 6720.
[37] P.J. Metaxas, Solid State Phys. 62 (2011) 76.
[38] L. Thevenard, C. Gourdon, S. Haghgoo, J.-P. Adam, H.J. von Bardeleben, A. Lemaire, W. Schoch, A. Thiaville, Phys. Rev. B 83 (2011) 245211.
[39] K. Yamada, J.-P. Jamet, Y. Nakatani, A. Mougin, A. Thiaville, T. Ono, J. Ferré, Appl. Phys. Express 4 (2011) 113001.
[40] B. Van de Viel, L. Laurson, G. Durin, Phys. Rev. B 86 (2012) 144415.
[41] J. Ferré, in: B. Hillebrands, K. Ounadjela (Eds.), Spin Dynamics in Confined Magnetic Structures I, in: Topics in Applied Physics, vol. 83, Springer-Verlag, Berlin, Heidelberg, 2002, pp. 127–165.
[42] A. Kirilyuk, J. Ferré, J. Pommier, D. Renard, J. Magn. Magn. Mater. 121 (1993) 536.
[43] A. Kirilyuk, J. Ferré, D. Renard, IEEE Trans. Magn. 29 (1993) 2518.
[44] M. Müller, D.A. Gorochov, G. Blatter, Phys. Rev. B 63 (2001) 184305.
[45] T. Giamarchi, A.B. Kolton, A. Rosso, Lect. Notes Phys. 688 (2006) 91.
[46] S. Bustingorry, A.B. Kolton, T. Giamarchi, Europhys. Lett. 81 (2008) 26005.
[47] A.B. Kolton, A. Rosso, T. Giamarchi, W. Krauth, Phys. Rev. B 79 (2009) 184207.
[48] J.-C. Lee, K.-J. Kim, J. Ryu, K.-W. Moon, S.-J. Yun, G.-H. Gim, K.-S. Lee, K.-H. Shin, H.-W. Lee, S.-B. Choe, Phys. Rev. Lett. 107 (2011) 067201.
[49] S. Bustingorry, A.B. Kolton, T. Giamarchi, Phys. Rev. B 85 (2012) 214416.
[50] W. Kleemann, J. Rheusius, O. Petrovic, J. Ferré, J.-P. Jamet, H. Bernas, Phys. Rev. Lett. 99 (2007) 097203.
[51] J. Ferré, in: G.C. Hadjipanayis (Ed.), Magnetic Storage Systems Beyond 2000, Kluwer Academic Publishers, Dordrecht, The Netherlands, 2001, p. 181.
[52] J.P. Attané, M. Tissier, A. Marty, L. Vila, Phys. Rev. B 82 (2010) 024408.
[53] T. Nattermann, V. Pokrovsky, V.M. Vinokur, Phys. Rev. Lett. 87 (2001) 197005.
[54] A.B. Kolton, A. Rosso, T. Giamarchi, W. Krauth, Phys. Rev. Lett. 97 (2006) 057001.
[55] J. Gorchon, S. Bustingorry, J. Ferré, V. Jeudy, A.B. Kolton, T. Giamarchi, submitted for publication.
[56] E. Agoritsas, V. Lecomte, T. Giamarchi, Phys. Rev. B 82 (2010) 184207.
[57] S. Emori, G.S.D. Beach, J. Phys. Condens. Matter 24 (2012) 024214.
[58] G. Rodriguez-Rodriguez, J.L. Menendez, A. Hierro-Rodriguez, A. Pérez-Junquera, N. Montenegro, D. Ravelosona, J.M. Alameda, M. Vélez, J. Phys. D, Appl. Phys. 43 (2010) 305002.
[59] A. Kirilyuk, J. Ferré, D. Renard, Europhys. Lett. 24 (1993) 403.
[60] J. Ferré, V. Repain, J.-P. Jamet, A. Mougin, V. Mathet, C. Chappert, H. Bernas, Phys. Status Solidi A 201 (2004) 1386.
[61] J. Ferré, J.-P. Jamet, in: H. Kronmüller, S. Parkin (Eds.), Handbook of Magnetism and Advanced Magnetic Materials, vol. 3, Novel Techniques for Characterizing and Preparing Samples, John Wiley & Sons, 2007, p. 1710.
[62] F. Cayssol, J.L. Menendez, D. Ravelosona, C. Chappert, J.-P. Jamet, J. Ferré, H. Bernas, Appl. Phys. Lett. 86 (2005) 022503.
[63] J.H. Franken, H.J.M. Swagten, B. Koopmans, Nat. Nanotechnol. 7 (2012) 499.
[64] L. Krusin-Elbaum, T. Shibauchi, B. Argyle, L. Gignac, D. Weller, Nature 410 (2001) 444.
[65] M. Bauer, A. Mougin, J.-P. Jamet, V. Repain, J. Ferré, R.L. Stamps, H. Bernas, C. Chappert, Phys. Rev. Lett. 94 (2005) 207211.
[66] T. Shibauchi, L. Krusin-Elbaum, V.M. Vinokur, B. Argyle, D. Weller, B.D. Terris, Phys. Rev. Lett. 87 (2001) 267201.
[67] P.J. Metaxas, R.L. Stamps, J.-P. Jamet, J. Ferré, V. Baltz, B. Rodmacq, J. Phys. Condens. Matter 24 (2012) 024212.
[68] J. Moritz, F. Garcia, J.C. Toussaint, B. Dieny, J.P. Nozières, Europhys. Lett. 65 (2004) 123.
[69] V. Grolier, D. Renard, B. Bartenlian, P. Beauvillain, C. Chappert, C. Dupas, J. Ferré, M. Galtier, E. Kolb, M. Mulloy, J.P. Renard, P. Veillet, Phys. Rev. Lett. 71 (1993) 3023.
[70] P.J. Metaxas, J.-P. Jamet, J. Ferré, B. Rodmacq, B. Dieny, R.L. Stamps, J. Magn. Magn. Mater. 320 (2008) 2571.
[71] P.J. Metaxas, R.L. Stamps, J.-P. Jamet, J. Ferré, V. Baltz, B. Rodmacq, P. Politi, Phys. Rev. Lett. 104 (2010) 237206.
[72] P. Politi, P.J. Metaxas, J.-P. Jamet, R.L. Stamps, J. Ferré, Phys. Rev. B 84 (2011) 054431.
[73] S. Fukami, T. Suzuki, K. Nagahara, N. Ohshima, Y. Ozaki, S. Saito, R. Nebashi, N. Sakimura, H. Honjo, K. Mori, C. Igarashi, S. Miura, N. Ishiwata, T. Sugibayashi, Low-current perpendicular domain wall motion cell for scalable high-speed MRAM, in: Symposium on VLSI Technology, 2009.
[74] S.S.P. Parkin, M. Hayashi, L. Thomas, Science 320 (2008) 190.
[75] F. Cayssol, D. Ravelosona, C. Chappert, J. Ferré, J.-P. Jamet, Phys. Rev. Lett. 92 (2004) 107202.
[76] B. Derrida, J. Stat. Phys. 31 (1983) 433.
[77] D.A. Allwood, G. Xiong, D. Cooke, C.C. Faulkner, D. Atkinson, N. Vernier, R.P. Cowburn, Science 296 (2002) 2003.
[78] D.A. Allwood, G. Xiong, C.C. Faulkner, D. Atkinson, D. Petit, R.P. Cowburn, Science 309 (2005) 1688.
[79] J. Grollier, A. Chathboula, R. Matsumoto, A. Anane, V. Cros, F. Nguyen van Dau, A. Fert, C. R. Physique 12 (2011) 309.
[80] G. Malinovski, O. Boulle, M. Käui, J. Phys. D, Appl. Phys. 44 (2011) 384005.
[81] I.M. Miron, T. Moore, H. Szambolics, L.D. Buda-Prejbeanu, S. Auffret, B. Rodmacq, S. Pizzini, J. Vogel, M. Bonfim, A. Schuhl, G. Gaudin, Nat. Mater. 10 (2011) 419.
[82] G.S.D. Beach, C. Knutson, C. Nistor, M. Tsoi, J.L. Erskine, Phys. Rev. Lett. 97 (2006) 057203.
[83] S.-W. Jung, W. Kim, T.-D. Lee, K.-J. Lee, H.-W. Lee, Appl. Phys. Lett. 92 (2008) 202508.
[84] S. Fukami, T. Suzuki, N. Ohshima, K. Nagahara, N. Ishiwata, J. Appl. Phys. 103 (2008) 07E718.
[85] K.-J. Kim, J.-C. Lee, K.-H. Shin, H.-W. Lee, S.-B. Choe, Curr. Appl. Phys. 13 (2013) 228.

[86] Yamanouchi, D. Chiba, F. Matsukura, H. Ohno, Nature 428 (2004) 539.
[87] J.P. Adam, N. Vernier, J. Ferré, A. Thiaville, V. Jeudy, A. Lemaitre, L. Thevenard, G. Faini, Phys. Rev. B 80 (2009) 193204.
[88] J. Heinen, O. Boulle, K. Rousseau, G. Malinovski, M. Kläui, H.J.M. Swagten, B. Koopmans, C. Ulysse, G. Faini, Appl. Phys. Lett. 96 (2010) 202510.
[89] R. Lavrijsen, P.P.J. Haazen, E. Murè, J.H. Franken, J.T. Kohlhepp, H.J.M. Swagten, B. Koopmans, Appl. Phys. Lett. 100 (2012) 262408.
[90] M. Cormier, A. Mougin, J. Ferré, A. Thiaville, N. Charpentier, F. Piéchon, R. Weil, V. Baltz, B. Rodmacq, Phys. Rev. B 81 (2010) 024407.
[91] D. Ravelosona, D. Lacour, J.A. Katine, B.D. Terris, C. Chappert, Phys. Rev. Lett. 95 (2005) 117203.
[92] D. Ravelosona, S. Mangin, J.A. Katine, E.E. Fullerton, B.D. Terris, Appl. Phys. Lett. 90 (2007) 072508.
[93] C. Burrowes, A.P. Mihai, D. Ravelosona, J.-V. Kim, C. Chappert, L. Vila, A. Marty, Y. Samson, F. Garcia-Sanchez, L.D. Buda-Prejbeanu, I. Tudosa, E.E. Fullerton, J.-P. Attané, Nat. Phys. 6 (2010) 17.
[94] L. Liu, O.J. Lee, T.J. Gudmundsen, D.C. Ralph, R.A. Buhrman, Phys. Rev. Lett. 109 (2012) 096602.
[95] A. Thiaville, S. Rohart, E. Jué, V. Cros, A. Fert, Europhys. Lett. 100 (2012) 57002.
[96] L. San Emeterio Alvarez, K.-Y. Wang, S. Lepadatu, S. Landi, S.J. Bending, C.H. Marrows, Phys. Rev. Lett. 104 (2010) 137205.
[97] M. Yamanouchi, D. Chiba, F. Matsukura, T. Dietl, Phys. Rev. Lett. 96 (2006) 096601.
[98] K.-W. Moon, D.-H. Kim, S.-C. Yoo, C. -Gu Cho, S. Hwang, B. Kahng, B.-C. Min, K.-H. Shin, S.-B. Choe, Phys. Rev. Lett. 110 (2013) 107203.
[99] J. Ryu, S.-B. Choe, H.-W. Lee, Phys. Rev. B 84 (2011) 075469.
[100] V. Lecomte, S.E. Barnes, J.-P. Eckmann, T. Giamarchi, Phys. Rev. B 80 (2009) 054413.
[101] P.J. Metaxas, P.-J. Zermatten, J.-P. Jamet, J. Ferré, G. Gaudin, B. Rodmacq, A. Schuhl, R.L. Stamps, Appl. Phys. Lett. 94 (2009) 132504.
[102] P.J. Metaxas, P.-J. Zermatten, R.L. Novak, S. Rohart, J.-P. Jamet, R. Weil, J. Ferré, A. Mougin, R.L. Stamps, G. Gaudin, V. Baltz, B. Rodmacq, J. Appl. Phys. 113 (2013) 073906.
[103] A. Pérez-Junquera, V.I. Marconi, A.B. Kolton, L.M. Alvarez-Prado, Y. Souche, A. Alija, M. Vélez, J.V. Anguita, J.M. Alameda, J.I. Martin, J.M.R. Parrondo, Phys. Rev. Lett. 100 (2008) 037203.
[104] E.B. Kolomeisky, T. Curcic, J.P. Stralev, Phys. Rev. Lett. 75 (1995) 1775.
[105] A.M. Ettouhami, L. Radzihovsky, Phys. Rev. B 67 (2003) 115412.
[106] S. Bustingorry, A.B. Kolton, T. Giamarchi, Phys. Rev. B 82 (2010) 094202.